



HAL
open science

Direct comparison of ITS-90 and PLTS-2000 from 0.65 K to 1 K at LNE-CNAM

Changzhao Pan, Fernando Sparasci, Mark Plimmer, Lara Risegari,
Jean-Michel Daugas, Gérard Rouille, Bo Gao, Laurent Pitre

► To cite this version:

Changzhao Pan, Fernando Sparasci, Mark Plimmer, Lara Risegari, Jean-Michel Daugas, et al.. Direct comparison of ITS-90 and PLTS-2000 from 0.65 K to 1 K at LNE-CNAM. *Metrologia*, 2021, 58 (2), pp.025005. 10.1088/1681-7575/abd845. hal-03672163

HAL Id: hal-03672163

<https://cnam.hal.science/hal-03672163>

Submitted on 19 May 2022

HAL is a multi-disciplinary open access archive for the deposit and dissemination of scientific research documents, whether they are published or not. The documents may come from teaching and research institutions in France or abroad, or from public or private research centers.

L'archive ouverte pluridisciplinaire **HAL**, est destinée au dépôt et à la diffusion de documents scientifiques de niveau recherche, publiés ou non, émanant des établissements d'enseignement et de recherche français ou étrangers, des laboratoires publics ou privés.



Distributed under a Creative Commons Attribution 4.0 International License



PAPER • OPEN ACCESS

Direct comparison of ITS-90 and PLTS-2000 from 0.65 K to 1 K at LNE-CNAM

To cite this article: Changzhao Pan *et al* 2021 *Metrologia* **58** 025005

View the [article online](#) for updates and enhancements.

You may also like

- [Progress towards a new definition of the kelvin](#)
Joachim Fischer
- [Comparison of the copper blackbody fixed-point cavities between NIS and LNE-Cnam](#)
M G Ahmed, K Ali, F Bourson *et al.*
- [The equilibrium liquidus temperatures of rhenium-carbon, platinum-carbon and cobalt-carbon eutectic alloys](#)
D H Lowe, A D W Todd, R Van den Bossche *et al.*

Direct comparison of ITS-90 and PLTS-2000 from 0.65 K to 1 K at LNE-CNAM

Changzhao Pan^{1,2}, Fernando Sparasci^{1,2,*}, Mark Plimmer^{1,2},
Lara Risegari¹, Jean-Michel Daugas¹, Gérard Rouille³, Bo Gao^{2,4}
and Laurent Pitre^{1,2,*}

¹ LCM-LNE-Cnam, 61 rue du Landy, 93210 La Plaine-Saint Denis, France

² TIPC-LNE Joint Laboratory on Cryogenic Metrology Science and Technology, Technical Institute of Physics and Chemistry (TIPC), Chinese Academy of Sciences (CAS), Beijing 100190, People's Republic of China

³ Institut d'Astrophysique Spatiale - Université Paris-Sud, 91405 Orsay CEDEX, France

⁴ Key Laboratory of Cryogenics, Technical Institute of Physics and Chemistry, Chinese Academy of Sciences, Beijing, 100190, People's Republic of China

E-mail: laurent.pitre@cnam.fr and fernando.sparasci@lecnam.net

Received 12 October 2020, revised 20 December 2020

Accepted for publication 4 January 2021

Published 19 February 2021



CrossMark

Abstract

In the temperature range between 0.65 K and 1 K, the international temperature scale of 1990 (ITS-90) is based on ³He vapour–pressure thermometers and overlaps with the provisional low temperature scale of 2000 (PLTS-2000) defined by the melting pressure of ³He. An *indirect* comparison at PTB revealed differences between the two scales of up to 1.5 mK at 0.65 K (Engert *et al* 2007 Metrologia **44** 40–52). Stimulated by the PTB results, we have performed a *direct* comparison $T_{90}-T_{2000}$ from 0.65 K to 1 K at LNE-CNAM. To test repeatability, the experiment was conducted twice: in 2019 and 2020. We find differences $T_{90}-T_{2000}$ of 0.28 mK at 1 K, increasing to 1.58 mK at 0.65 K. The direct comparison, eliminates the uncertainty component due to the transfer resistance thermometer and its calibration. Except for a point near 1 K, the new results are in accordance with those obtained at PTB (differences of less than 0.22 mK), which makes it possible to improve the accuracy of the equation specified in ITS-90.

Keywords: international temperature scale of 1990 (ITS-90), provisional low temperature scale of 2000 (PLTS-2000), vapour pressure of ³He, melting curve of ³He, low temperature thermometry

1. Introduction

Two different international temperature scales are employed for thermometry in the temperature range 0.65 K–1 K: the international temperature scale of 1990 ITS-90 [1] and the provisional low temperature scale PLTS-2000 [2, 3].

In ITS-90, temperature is defined by the relationship between vapour pressure and temperature of helium-3 (³He) liquid/vapour interface. The equation is based on the work of Rusby and Swenson [4] and El Samahy [5] using the extrapolation of magnetic salt thermometry and its reference from the constant-volume gas thermometry of Berry [6]. For PLTS-2000, temperature is defined by the relationship between melting pressure and temperature of ³He. The equation is based on the background data of Soulen *et al* from NIST [7], Schuster *et al* from PTB [8] and Ni *et al* from University of Florida [9] and a thermodynamic analysis as detailed in Rusby *et al* [3]. For temperatures down to 20 mK, the agreement between the two laboratories is excellent.

* Authors to whom any correspondence should be addressed.

 Original content from this work may be used under the terms of the [Creative Commons Attribution 4.0 licence](https://creativecommons.org/licenses/by/4.0/). Any further distribution of this work must maintain attribution to the author(s) and the title of the work, journal citation and DOI.

Since the adoption of the ITS-90 and PLTS-2000, several national laboratories have set up apparatus to implement them at temperatures below 1.0 K. The following is a short review of work on both scales.

As far as ITS-90 is concerned, in 1996, Meyer and Reilly at NIST [10] reported results for the range of 0.65 K–5.0 K. Comparing ITS-90 to the NIST wire scale (T_{NIST} , traceable to T_{X1} [4]), they found a difference of about 0.9 mK at 0.65 K. In 1997, M.J. De Groot at NMi-VSL [11] established ITS-90 in the same temperature range. In 2002, as part of an international comparison, Hill at NRC [12] reported results for ITS-90 below 4.2 K. In 2003 Shimazaki and Tamura at NMIJ/AIST [13] implemented ITS-90 between 0.65 K and 3 K before upgrading their apparatus to a cryogen-free system in 2011 [14]. In 2003, Engert and Fellmuth at PTB [15] reported extensive measurements of ^3He vapour pressure from 0.65 K to 1.2 K. Later, in 2007, using PLTS-2000 to estimate the thermodynamic inconsistency of ITS-90 below 1 K, Engert *et al* [16] established a new ^3He vapour pressure scale known as PTB-2006.

PLTS-2000 is based to a large extent on the work of Schuster *et al* [17] which led to the creation of the ultra-low temperature scale PTB-1996. Subsequently, in 2013, Engert *et al* [18] reported the realization, maintenance and dissemination of PLTS-2000 in the same laboratory.

In 2003, Peruzzi and De Groot [19] evaluated the uncertainty in the realization of the PLTS-2000 from 10 mK to 1 K at the NMi-VSL. In the same year, one of us (LP) and two colleagues [20, 21] realized PLTS-2000 in the temperature range from 20 mK to 1 K and compared PLTS-2000 with a second sound thermometer at BNM-INM (presently LNE-CNAM). Finally, in 2016, Nakagawa [22] reported the implementation of PLTS-2000 below 0.65 K for calibration services at NMIJ/AIST.

From the brief review above, it can be seen that very few laboratories can implement both ITS-90 and PLTS-2000 from 0.65 K to 1 K, while only PTB has intercompared the two scales in this temperature range. The PTB's results showed that the inconsistencies between them increase from 0.66 mK at 1 K to 1.51 mK at 0.65 K. Of the two scales, PLTS-2000 has a sounder thermodynamic basis and the potential for a lower uncertainty. For this reason, to establish a harmonious connection between them, it has been suggested that values of PLTS-2000 should be used to correct ITS-90 rather than the reverse [15, 16]. To this end, PTB has carried out such a task, performing an indirect comparison in 2006 [16] in which two rhodium-iron resistance thermometers were used as transfer standards.

To establish a *direct* link between the ITS-90 and the PLTS-2000, since 2011, our group at LNE-CNAM has been using respectively a ^3He vapour pressure thermometer (VPT) combined with a ^3He melting pressure thermometer (MPT) in a commercial dilution refrigerator [23]. This paper presents the latest results of such a direct comparison $T_{90}-T_{2000}$ from 0.65 K to 1 K we carried out in 2019 and 2020.

The rest of the paper is structured as follows. In section 2, the experimental set-up is presented, which includes the cryostat, the gas processing system and the measurement

of the ^3He melting pressure and ^3He vapour pressure. In section 3, values of $T_{90}-T_{2000}$ are presented together with their uncertainties.

2. Experimental set-up

2.1. Cryostat

The cryostat used in this work was described in detail in our earlier article on the same subject [23]. Shown in figure 1, it is based on a commercial dilution refrigerator and uses liquid helium as the cryogen. All parts of the cryostat below 4 K are in a high-vacuum chamber (operating pressure below 1×10^{-5} Pa). The MPT sensing element and the VPT cell are installed on the same copper platform at the bottom. The platform has nine wells for the calibration of rhodium-iron thermometers. The working temperature on the surface of the platform is regulated by a Cernox[®] thermometer and heater, controlled using a proportional-integral-differential (PID) feedback loop written in LabVIEW[®] software. The temperature stability indicated by the standard deviation of the rhodium-iron thermometer reading is better than 0.1 mK (over several hours). Since the lowest achievable temperature with the cryostat, 20 mK, lies well below that of the melting pressure minimum (315.24 mK), the apparatus can be used to measure the minimum pressure of the melting pressure thermometer for the calibration of the *in situ* transducer (see section 3.1).

To reduce the thermal load on the lower copper platform, the pressure tubes of MPT and VPT are thermally connected to the still and mixing chamber flanges they traverse. A long stainless-steel capillary is used for the pressure tube of the melting pressure thermometer. To facilitate the calculation of the hydrostatic pressure correction of the MPT, the first section of this capillary is installed inside a vacuum tube, as shown in figure 1, and a heater is used to warm it up to room temperature during the calibration process. The temperature gradient between room temperature and 4.2 K occurs, by construction, along a horizontal capillary. The VPT tube is illustrated in our previous article [23]. Also, to simplify the calculation of the hydrostatic pressure correction, vertical segments are made of (high thermal conductivity) copper tubing below the 4 K flange. In addition, to reduce the thermomolecular effect, a tube diameter of 36 mm is used between the part of the tube at 30 K and the flanges at room temperature. It has a vacuum sleeve to isolate it from the liquid helium bath.

2.2. Gas handling systems

The apparatus is equipped with two separate gas handling systems: one for the MPT (PLTS-2000), the other for the VPT (ITS-90). Here below is a short description of both.

2.2.1. MPT gas handling system to implement PLTS-2000.

Figure 2 shows the gas handling system for the melting pressure thermometer. Normally, the gaseous ^3He is stored in a big dump at a pressure lower than atmospheric pressure to prevent its leaking to atmosphere. During the experiment, the ^3He gas

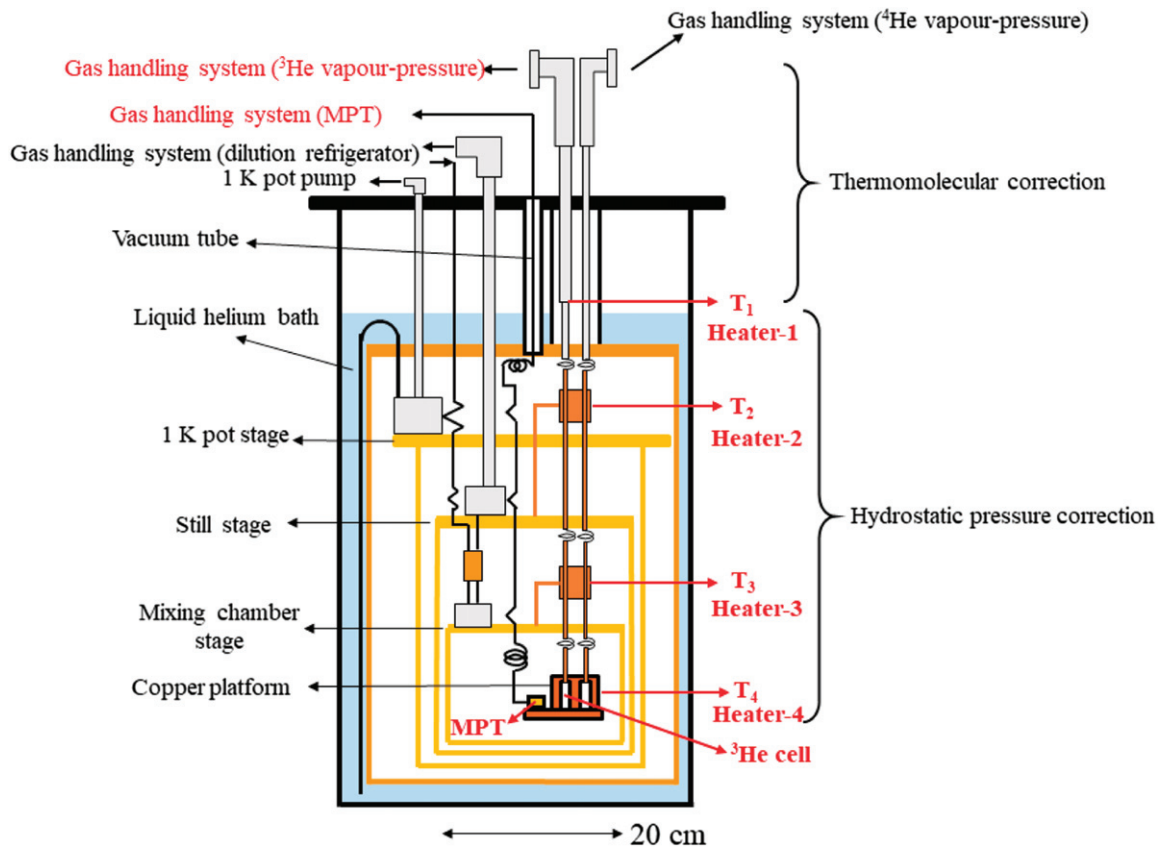


Figure 1. The cryostat used for the comparison of the temperature scales ITS-90 and PLTS-2000. MPT: melting-pressure thermometer. The gas handling system for ^4He is not used in the present work. For a detailed description see Sparasci *et al* (2011) [23]. For convenience, the vertical scale has been compressed.

is first pumped out from the dump by the liquid helium cold trap (labelled ‘HP cold trap’ in figure 2). The trap is then placed in a liquid nitrogen Dewar vessel. We control the pressure inside the gas treatment system by manually inserting this cold trap into the liquid nitrogen (LN_2) Dewar vessel or withdrawing it. The gas treatment system includes another cold trap, which is used to remove impurities condensable by LN_2 . Such a system is usually sufficient to remove impurities from the ^3He sample. A second capillary identical to the first is installed in parallel between the gas handling system and the 4 K flange. It is kept only as a backup in case the main capillary becomes blocked by condensed residual impurities.

The pressure at the top of the cryostat, where ^3He is at room temperature, is measured by a digital resonant quartz gauge (Paroscientific Digiquartz® model 1000, range 0–6.8 MPa absolute), named DQ_{MPT} hereafter. It is installed in an oil bath and its temperature is stabilized around 30 °C, the maximum excursion never exceeding ± 5 mK over 120 h. The corresponding standard deviation is 1.5 mK.

The pressure of the ^3He melting pressure is measured with a capacitive pressure transducer manufactured and initially tested by PTB [24] (named MPT in figure 2(a)). A commercial bridge (Andeen–Hagerling, model 7500A) is used to measure the capacitance of this transducer during the experiment. The DQ_{MPT} cannot be used to measure the pressure in the MPT during operation because there is a mixture of solid

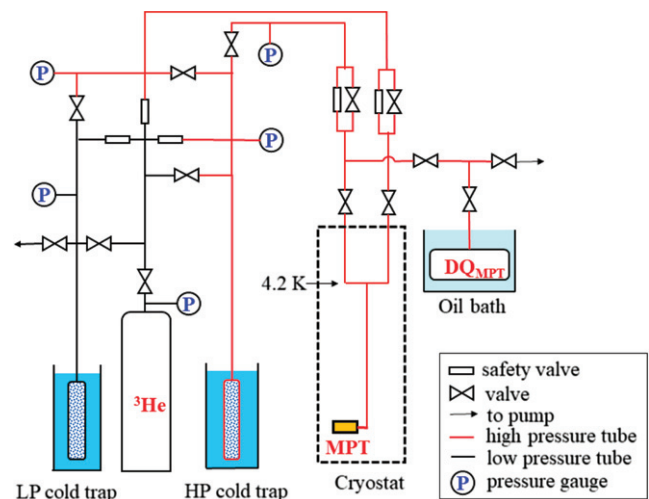


Figure 2. Gas handling system for the melting pressure thermometer. DQ_{MPT} : digital resonant quartz manometer; HP: high pressure; LP: low pressure.

and liquid ^3He in the filling line. For this reason, the MPT was designed to include a built-in capacitive pressure sensor, which must first be calibrated *in situ* at a temperature higher than 1 K, i.e. when all the ^3He in the filling line is in liquid form.

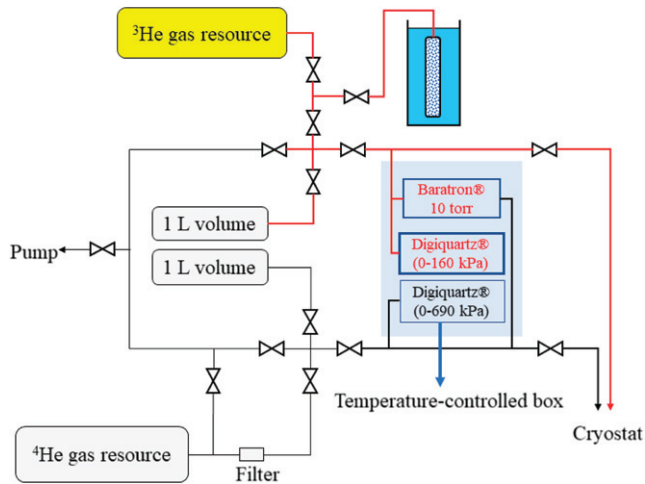


Figure 3. Gas handling system for ^3He vapour–pressure measurements (red lines). The 1 L volumes are used to estimate the amount of helium in either or both of the evaporators, this volume being a few times greater than that of the rest of the tubing.

2.2.2. VPT gas handling system for implementation of ITS-90.

Figure 3 shows the gas handling system of the vapour pressure thermometer. It contains a ^3He part and a ^4He part (though the latter is not used in the experiment described here). Both are similar except that the ^3He part has a liquid helium cold trap to remove liquid and gaseous ^3He from the experimental VPT cell. The specified purity of the ^3He is 99.996%. The effect of an impurity at the 10 ppm level is less than 0.01 mK [16, 25]. All pressure sensors are installed in a temperature-controlled commercial stainless-steel box (Measurements International, Model 9300A) equipped with an electromagnetic shield, inside which the temperature is controlled to within a maximum excursion of 50 mK around a given set point.

The pressure sensor used in this experiment is a high-precision differential capacitance manometer (MKS Baratron 698A 10 Torr), hereafter referred to as CM_{VPT} , which has been calibrated by direct comparison with the piston manometer FPG8601 in the range of 0–1300 Pa. The calibration is traceable to the French national standard and guarantees the link of the calibration results to the international system of units (SI).

3. Pressure measurement procedures

This section provides details on the procedures employed for accurate pressure measurements with both the MPT and the VPT.

3.1. MPT pressure measurements

Prior to the experiment, the relationship between the MPT measured capacitance, C , and the pressure, p , is determined by a two-step calibration process. In the first step, a calibrated piston balance (Ruska 2465A) is employed to calibrate DQ_{MPT} between 2.9 MPa and 4.1 MPa. In the second step, DQ_{MPT} is used to transfer the pressure calibration to the *in situ* capacitive pressure transducer in the MPT, via the Andeen-Hagerling

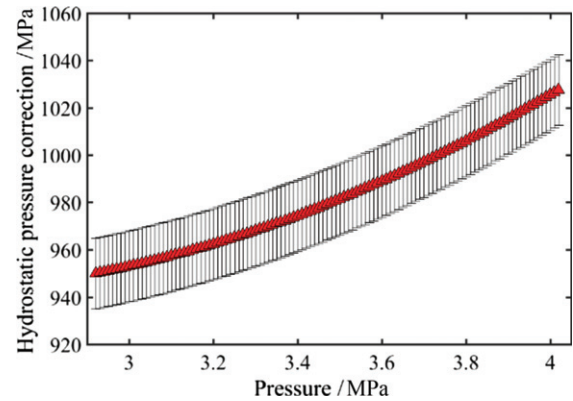


Figure 4. The hydrostatic pressure correction of the ^3He melting pressure thermometer during calibration at 1.2 K, together with standard uncertainty bars.

capacitance bridge. Throughout the second step, the temperature of the capacitive pressure transducer is kept close to 1.2 K, as prescribed in [20, 26].

The C versus p relationship obtained after this two-step calibration process is affected by an overall pressure offset which is the sum of two main contributions. One is the hydrostatic pressure generated by the gas column filling the capillary used to connect DQ_{MPT} with the capacitive pressure transducer. The hydrostatic pressure is caused by the difference in height and density between the DQ_{MPT} and the capacitance pressure transducer, the density difference being due to the temperature differential. (We recall the former is at 303 K and the latter at 1.2 K). For pressures between 2.9 MPa and 4.1 MPa, the hydrostatic pressure correction is a monotonically increasing function of pressure and can be calculated using the model provided in reference [19]. Figure 4 shows the trend of the hydrostatic pressure correction and the associated standard uncertainties. The latter amount to 15 Pa, as reported previously [20].

The second offset contribution comes from the quartz transducer DQ_{MPT} . As shown below in section 3.1.1, it is nearly constant over the whole pressure range. Consequently, the overall pressure offset is also a monotonically increasing function of pressure, with the same trend as the hydrostatic pressure function. As recommended in [19], its minimum value can be evaluated by measuring the MPT capacitance at the known minimum of the melting pressure, at 2.93113 MPa [3]. Thereafter, it can be calculated at any other pressure up to 4.1 MPa and removed in post-processing. The evaluation of the pressure minimum in the experiment reported in this paper is discussed in section 3.1.2.

Finally, another phenomenon affecting measurement quality is the hysteresis of the melting pressure capacitive sensor, mentioned in our paper of 2003 [20]. This point and the technique employed to reduce the hysteresis are discussed below in section 3.1.3.

3.1.1. DQ_{MPT} stability. The invariance of the DQ_{MPT} offset between 2.9 MPa and 4.1 MPa is apparent from the history of its calibrations carried out with the piston balance in 2001, 2015 and 2017. Figure 5 shows the pressure offset from

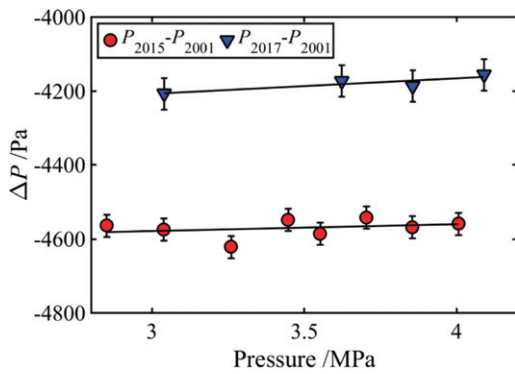


Figure 5. Offset of DQ_{MPT} with respect to its 2001 value, checked in 2015 (lower circles) and 2017 (upper triangles). The solid lines are least-squares fits to a linear function (slopes given in text).

the 2001 calibration. One sees that the offset pressure values lie around an almost horizontal straight line: slope 19 ± 23 Pa/MPa in 2015 and 42 ± 14 Pa/MPa in 2017, for the pressure range from 3.22 MPa to 4 MPa, corresponding to ^3He melting temperatures between 0.65 K and 1.00 K. We consider that such a long-term stability results from the fact that the gauge has been kept immersed for nearly 20 years in the temperature-controlled oil bath shown in figure 2. Due to technical difficulties, it was not possible to re-calibrate DQ_{MPT} in 2019 nor in 2020. However, since the storage conditions were identical to those of the period 2001–2017 and the sensor was neither used for other experiments, nor removed from the MPT gas handling system, we assume its behaviour also remained unchanged between 2017 and 2020. For the measurements presented in this paper, the DQ_{MPT} offset slope is thus taken to be almost vanishing between 3.22 MPa and 4 MPa, to within 36 Pa, while the offset value is determined measuring the ^3He melting pressure minimum, as described above.

3.1.2. MPT pressure minimum measurement. The MPT pressure minimum is used to estimate the overall offset affecting the C versus p relationship of the MPT, as mentioned above. Figure 6 shows the minima of the melting pressure observed in the 2019 and 2020 experiments.

To obtain a stable MPT pressure minimum, the temperature is twice swept upwards and downwards around it, as recommended in [19]. In 2019, the pressure minimum was located using single temperature sweeps of about 1.5 mK. In 2020, a double-sweep procedure was used: the first sweep used 2.5 mK temperature steps while the second sweep used steps half the size. Finally, the pressure minimum of the melting pressure could be located to within ± 10 Pa.

3.1.3. MPT capacitive sensor hysteresis. The hysteresis of the melting pressure capacitive sensor, mentioned in our paper of 2003 [20], is a phenomenon with an amplitude strongly correlated with the cooling process. In the 2019 experiment, there is a clear hysteresis when data are fitted using an eighth-order polynomial equation, as shown in figure 7. Such a high order is necessary when a large hysteresis is present. Yet, as

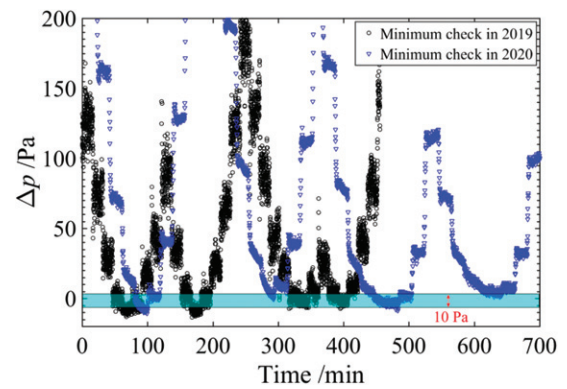


Figure 6. Minima of the melting pressure recorded by sweeping the temperature upwards and downwards (*sic*). The reference of the pressure deviations is the exact pressure minimum at 2.93113 MPa as recommended in [20].

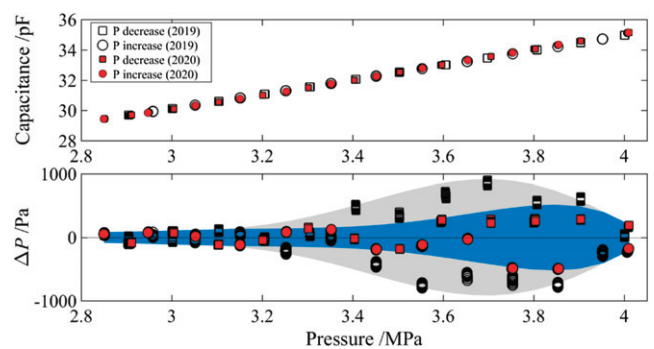


Figure 7. The graph in the upper part of the figure shows the capacitance measured as a function of the applied pressure at 1.2 K in 2019 and 2020. The lower part shows the corresponding fitting residuals of the eighth-order calibration polynomial. The blue and light grey shaded regions show the estimated uncertainty due to the hysteresis of the MPT capacitance gauge.

shown in the same paper [20], a lower-order polynomial provides a satisfactory fit when there is less hysteresis. To reduce the hysteresis in the 2020 experiment, an adjustment process was carried out. Before it was cooled down to below 4.2 K, the capacitance gauge was subjected to 20 pressure cycles between 2.8 MPa and 4.0 MPa at 77 K. Then, prior to the final calibration, it was given 20 more pressure cycles at 1.3 K. Figure 7 shows the impact of this procedure, which reduced the hysteresis twofold. Even so, some capacitor hysteresis remained.

3.2. VPT pressure measurements

The main uncertainty in the measurement of the ^3He vapour pressure comes from the calibration of the pressure sensor CM_{VPT} . Prior to vapour pressure measurements, two successive increases to the maximum pressure are performed to stabilize CM_{VPT} and check its correct operation. After this, the zero is adjusted immediately before the start of the measurements. During VPT measurements, the zero is checked regularly. During the measurements reported in this paper, no shift was observed at a level of 3 mPa.

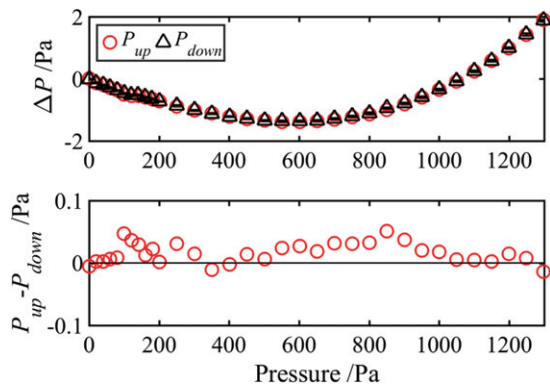


Figure 8. The calibration of the capacitance manometer CM_{VPT} (MKS Baratron 698A) used to measure ^3He pressure with respect to a piston balance (Fluke FPG8601) traceable to the French national standard.

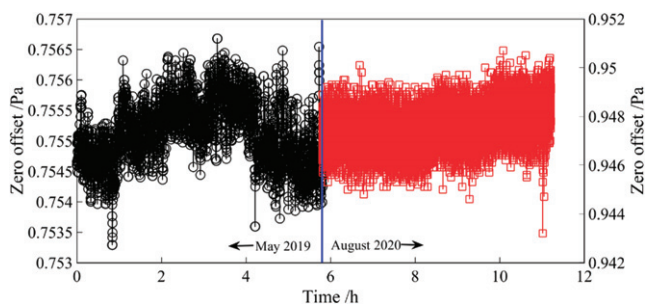


Figure 9. Zero offset of MKS Baratron 670B pressure gauge in May 2019 and August 2020.

Figure 8 shows the pressure differences between CM_{VPT} and the piston balance for both increasing and decreasing pressure. The hysteresis, less than 0.1 Pa, is included in the calibration uncertainty. The calibration was carried out in October 2019, i.e. between the time of the experiments in 2019 and 2020, and the same values were used to analyze all the experimental data. As the calibration is always performed starting at zero pressure, the zero point must be checked during each experiment. Figure 9 shows the zero offset measured when both sides of CM_{VPT} are evacuated by the same turbomolecular pump and the residual pressure is lower than 10^{-4} Pa. The results show that respective zero offsets of 0.755 ± 0.001 Pa and 0.947 ± 0.001 Pa must be subtracted when the data of the 2019 and the 2020 runs are analyzed.

Because the vapour pressure sensor CM_{VPT} is located at room temperature, while the ^3He cell is at low temperature (0.65–1 K), a hydrostatic head correction needs to be estimated. This aspect is detailed in our previous work [23], where the hydrostatic pressure correction is estimated to be around 1350 ppm of the vapour pressure in our system. Such a pressure difference corresponds to a temperature difference of 0.28 mK. In addition, to measure the ^3He vapour pressure accurately, the effect of the ratio of atomic mean free path to tube diameter (i.e. the thermomolecular effect) must be calculated. Several different models have been proposed to quantify the effect. To reduce uncertainties due to discrepancies between

them, while at the same time minimizing the impact of the thermomolecular effect to begin with, we decided to use the largest possible tube diameter allowed by the size of the cryostat [23]. With our specially designed pressure tube, the maximum overall correction of the thermomolecular effect is of the order of 200 ppm at the lowest pressure (100 Pa). This pressure difference amounts to a temperature difference of 0.02 mK. To reduce further the uncertainty caused by both hydrostatic and thermomolecular corrections, the temperatures at four points along the pressure tube are constantly measured *in situ* during the vapour pressure measurement, using the thermometers labelled T_1 to T_4 in figure 1.

4. $T_{90}-T_{2000}$ and associated uncertainty budget

Here we describe the comparison of ITS-90 and PLTS-2000 followed by the uncertainty budget.

4.1. Experimental realization of $T_{90}-T_{2000}$

Since the experiment described in this paper is a *direct* comparison between T_{2000} and T_{90} , all the MPT and VPT measurements presented hereafter were conducted simultaneously. The control thermometer and the heater located on the copper platform housing the MPT and the VPT devices were used to set the platform temperature. Once a stable set point was reached, the MPT capacitance and the VPT pressure were recorded at the same time.

The initial ^3He filling pressure of the MPT determines the temperature range over which T_{2000} can be measured. To span the range from 0.65 K to 1.0 K, three different filling pressures were employed. Between 0.65 K and 0.80 K, a pressure 3.7 MPa of ^3He was used. From 0.80 K to 0.95 K, the filling pressure was 4.0 MPa. Finally, to go from 0.95 K up to 1.0 K, a filling pressure of 4.1 MPa was used. Each filling was performed by setting the temperature of the MPT capacitive sensor to 1.2 K.

On the side of the VPT, to determine the effect of heat fluxes on the pressure tube and thereby minimize their impact on $T_{90}-T_{2000}$, the temperature T_3 on the pressure tube (see figure 1) was set to different values, by changing the power supplied to heater 3. Figure 10 shows the results of heating. In the 2019 experiment, the value of $T_{90}-T_{2000}$ rose when the T_3 was increased from about 650 mK to 670 mK. The rise occurred because the temperature T_3 was too close to that of the lower copper platform, possibly owing to the presence of liquid ^3He on the surface of the VPT pressure tube, though this is difficult to prove *a posteriori*. Once T_3 was decreased, the difference $T_{90}-T_{2000}$ returned to its original value. This implied that if the temperature difference between T_3 and the copper platform were large enough, the heating effect on the VPT pressure tube would have practically no influence on the value of the difference $T_{90}-T_{2000}$. This hypothesis was also verified at the outset of the 2020 experiment, as shown on the bottom side of figure 10. Consequently, during the 2020 run, a temperature difference of at least 50 mK was maintained between T_3 and the copper platform.

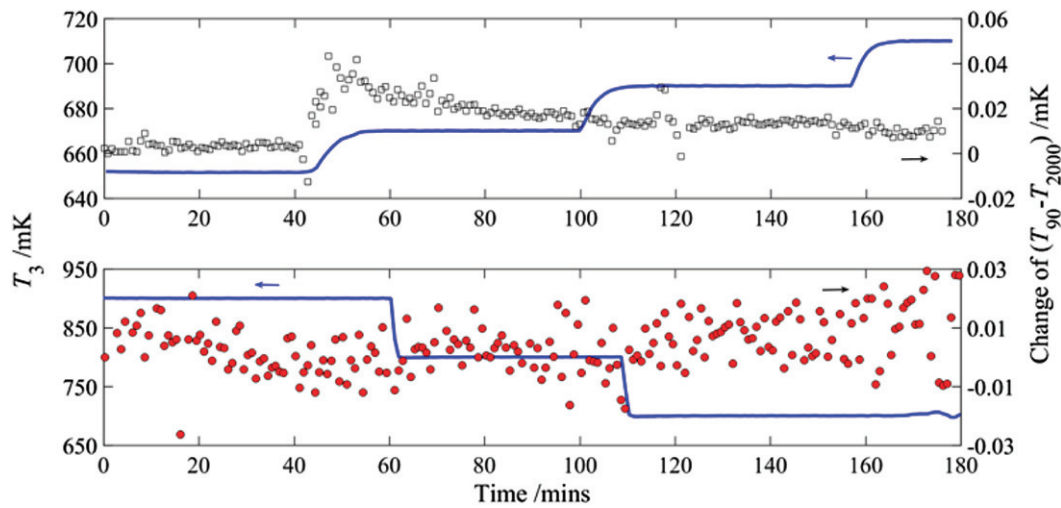


Figure 10. The effect of heating of the pressure tube on the value of the difference $T_{90}-T_{2000}$ at 650 mK. Top: heating steps applied for increasing temperature during run 1 (2019). Bottom: steps applied for decreasing temperature in run 2 (2020). The temperature T_3 (solid blue lines) corresponds to that of heater 3 shown in Figure 1. The difference in the sharpness of the steps between both figures is due to improved temperature regulation in the 2020 experiment.

Figure 11(a) shows typical results of $T_{90}-T_{2000}$ for the range 650 mK to 1 K. Results for 0.65 K are magnified in 11(b), where time is shown explicitly. One can see that $T_{90}-T_{2000}$ can be stable for several hours with a standard deviation of 5 μ K at 0.65 K. Such a stability boosts confidence in our results. Note that this stability is a product of the *direct* comparison between VPT and MPT. Due to oscillations of the PID temperature controller, the temperature of the copper platform housing the two thermometers shows variations larger than 5 μ K. When they are operated simultaneously, however, the VPT and the MPT measure the *same* temperature oscillations, which cancel out when the difference $T_{90}-T_{2000}$ is calculated. Had we used an indirect method with a calibrated transfer standard, we could not have removed the effect of these oscillations and the final spread of $T_{90}-T_{2000}$ values would have been significantly wider.

4.2. Uncertainty budget

Table 1 shows the uncertainty budget for $T_{90}-T_{2000}$ measurements, with the detail of components related to the melting pressure thermometer, the vapour–pressure thermometer and the temperature stability and gradient on the copper platform. The uncertainties given in table 1 are those pertaining to the second run, i.e. the experiment performed in 2020. Uncertainties of the first run (performed in 2019) are larger, owing essentially to the greater hysteresis in MPT measurements.

4.2.1. MPT uncertainties. The melting pressure thermometer uncertainty arises mainly from the calibration process. It includes several items. One is the hysteresis of the melting pressure measurement transducer (figure 7), which amounts to around 400 Pa. Another is the calibration of the quartz oscillator pressure transducer with respect to the pressure balance, which is typically 41 Pa [20]. The drift of the quartz oscillator pressure transducer accounts for less than 36 Pa,

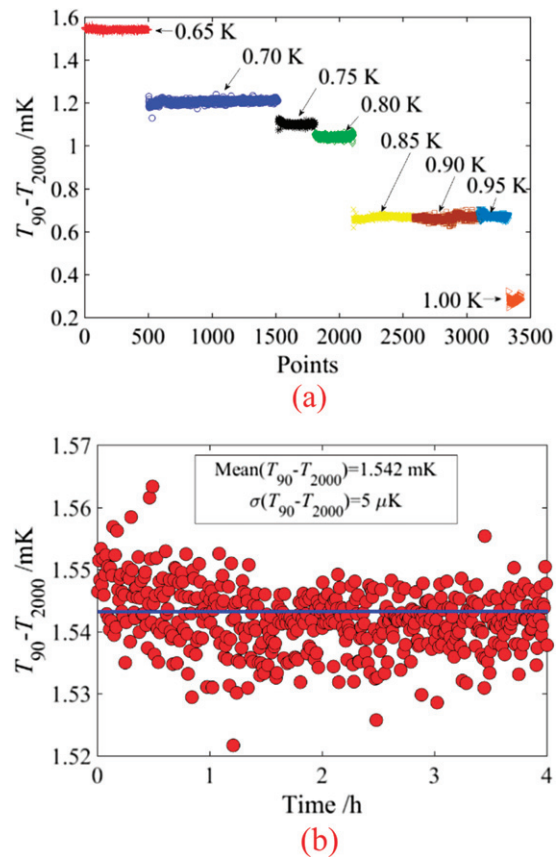


Figure 11. (a) The stability of $T_{90}-T_{2000}$ at each temperature point b) Enlargement for 650 mK. Note that data for each temperature were obtained on different days.

corresponding to the DQ_{MPT} offset slope (figure 5). The hydrostatic pressure correction amounts to less than 15 Pa while the adjustment of the calibration pressure to the melting pressure minimum adds less than 11 Pa.

Table 1. The uncertainty budget of $T_{90}-T_{2000}$ in the 2020 experiment (run 2). The word Baratron refers to the type of capacitance manometer. All values are in millikelvin.

Uncertainty component	T_{2000}							
	647.977	700.529	751.549	798.541	850.781	898.552	948.990	997.228
Melting pressure thermometer								
Hysteresis of the melting-pressure sensor	0.087	0.084	0.089	0.109	0.148	0.189	0.200	0.105
Calibration of quartz oscillator pressure transducer	0.025	0.023	0.021	0.019	0.018	0.017	0.016	0.015
Drift of quartz oscillator pressure transducer (slope)	0.022	0.020	0.018	0.017	0.016	0.015	0.014	0.013
Dielectric susceptibility of the epoxy	0.018	0.017	0.015	0.014	0.013	0.013	0.012	0.011
Capacitance bridge (linearity, stability but not accuracy)	0.010	0.010	0.010	0.010	0.010	0.010	0.010	0.010
^4He impurities in ^3He	0.012	0.012	0.012	0.012	0.012	0.012	0.012	0.012
Hydrostatic pressure correction	0.009	0.008	0.008	0.007	0.007	0.006	0.006	0.006
Adjustment of calibration pressure to the melting pressure minimum	0.007	0.006	0.005	0.005	0.004	0.004	0.004	0.004
Combined uncertainty for the MPT	0.098	0.093	0.097	0.114	0.151	0.191	0.203	0.109
Vapour–pressure thermometer								
Baratron calibration	0.056	0.040	0.031	0.025	0.020	0.017	0.014	0.013
Baratron zero offset and voltage auto-calibration	0.033	0.024	0.018	0.014	0.011	0.009	0.008	0.007
Hydrostatic pressure correction	0.022	0.014	0.016	0.017	0.019	0.02	0.022	0.021
Heating of tube	0.010	0.010	0.010	0.010	0.010	0.010	0.010	0.010
^4He impurities in ^3He	0.010	0.010	0.010	0.010	0.010	0.010	0.010	0.010
Thermo-molecular pressure difference	0.004	0.002	0.001	0.001	0.000	0.000	0.000	0.000
Combined uncertainty for the VPT	0.070	0.051	0.042	0.036	0.033	0.031	0.031	0.029
Other contributions								
Temperature differences in the experimental platform	0.010	0.010	0.010	0.010	0.010	0.010	0.010	0.010
Stability	0.005	0.009	0.008	0.006	0.008	0.011	0.009	0.011
Combined uncertainty	0.121	0.107	0.107	0.121	0.156	0.194	0.206	0.114

We also include uncertainties due to the temperature dependence of the dielectric susceptibility of the melting pressure sensor epoxy, the capacitance bridge and gas impurities (^4He gas in ^3He), all quantified in references [16, 26].

4.2.2. VPT uncertainties. The largest uncertainty component in the temperature measured by the vapour–pressure thermometer arises from the pressure uncertainty in the capacitance manometer calibration. The latter is drawn from the equation in the calibration certificate $u(p) = 0.059 \text{ Pa} + 8.3 \times 10^{-6}|p|$. The second largest contribution is related to the zero offset of the capacitance manometer CM_{VPT} , linked to the voltage self-calibration performed automatically by the sensor whenever the zero offset is determined. During the experiment, the zero offset with voltage self-calibration was checked several times, the maximum difference never exceeding 0.03 Pa. Another significant element comes from the correction of the hydrostatic pressure. As it is difficult to ascertain the exact height of the phase transition surface in the helium-3 cell, in the calculation of the hydrostatic pressure correction, half the height of the cell was used as a conservative estimate of the uncertainty.

The uncertainty in the second virial coefficient B of ^3He is also included in the uncertainty in the hydrostatic pressure correction. Thanks to progress in the most recent *ab initio* calculations [27–29], the value of B for temperatures above 1 K has now only a very small uncertainty. For temperatures below

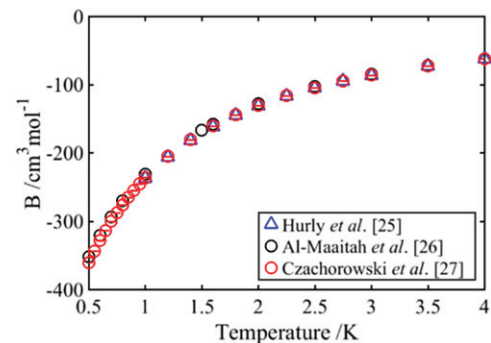


Figure 12. Values of the second virial coefficient B of ^3He at temperatures below 4 K from *ab initio* calculations. The agreement between three independent calculations is clearly excellent.

1 K, the results of Czachorowski *et al* (2020), Al-Maaitah *et al* (2017) and Hurly (2000) show a small difference (albeit less than 2% of the value of B), as shown in figure 12. Even so, overall, we find the uncertainty from B to be negligible.

The thermomolecular pressure difference also contributes to the uncertainty of the result. Referring to the CCT document [30], we have taken 20% of the value of the thermomolecular pressure difference as the uncertainty. The effect of heating shown in figure 10 and impurities in the ^3He are also included in the uncertainty budget.

Table 2. Differences $T_{90}-T_{2000}$ from 0.65 K to 1 K in the present work together with their combined standard uncertainty. All values are in millikelvin. Uncertainties are specified to two significant figures.

T_{2000}	Run-1		Run-2		Weighted average	
	$T_{90}-T_{2000}$	Uncertainty	$T_{90}-T_{2000}$	Uncertainty	$T_{90}-T_{2000}$	Uncertainty
647.9	1.630	0.15	1.542	0.12	1.577	0.094
700.5	1.329	0.19	1.219	0.11	1.245	0.093
751.5	1.053	0.25	1.101	0.11	1.094	0.098
798.5	0.913	0.32	1.042	0.12	1.026	0.11
850.7	1.000	0.36	0.666	0.16	0.718	0.14
898.5	0.843	0.35	0.664	0.19	0.706	0.17
948.9	0.599	0.27	0.674	0.21	0.647	0.16
997.2	—	—	0.281	0.11	0.281	0.11

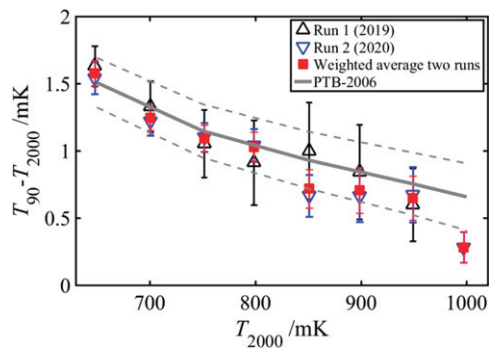


Figure 13. Values of $T_{90}-T_{2000}$ from 0.65 K to 1 K from the present work and a comparison with the results obtained at PTB in 2006 [16]. The dashed lines correspond to the combined standard uncertainty of PTB2006.

4.2.3. Other uncertainties. In addition to the aforementioned contributions, temperature gradients in the experimental platform can also influence the measured values of $T_{90}-T_{2000}$. As the locations of the melting pressure thermometer and the vapour pressure thermometer lie very close to each other, we have estimated the temperature difference to be no greater than 10 μ K. Lastly, fluctuations of $T_{90}-T_{2000}$ at each measuring point must be included. Typically, they never exceed 10 μ K, as shown in the example of figure 11. Since at this temperature, the Kapitza thermal resistance is very small [31], we assume that the thermal resistance contact between the liquid helium and the copper surface is negligible. Therefore, a temperature rise in the tube of the VPT has no effect upon the difference $T_{90}-T_{2000}$ as is clear from the graph of figure 10.

4.3. $T_{90}-T_{2000}$

Table 2 displays the results of the experiments of Run 1 in 2019 and Run 2 in 2020. The latter exhibit a lower uncertainty thanks to the reduced hysteresis of the MPT capacitance gauge. Final results for $T_{90}-T_{2000}$ from 0.65 K to 1 K are obtained from the weighted average of results from both runs.

Figure 13 shows all the results of both runs and their weighted average value. The uncertainty bars correspond to the standard uncertainties (coverage factor $k = 1$) associated with each measurement. The present results compare favourably

with those of the pioneering indirect comparison made at PTB in 2006 [15]. Except for the point around 1 K, all differences are below 0.22 mK and lie within the error bands of each laboratory's results.

5. Conclusion and perspectives

Practical thermometry traceable to the SI unit kelvin at temperatures below 1 K is based on either the international temperature scale of 1990 (ITS-90) or the provisional low temperature scale of 2000 (PLTS-2000), though the two scales differ slightly. In this region, ITS-90 uses the vapour pressure curve of liquid ^3He while PLTS-2000 is based on the melting pressure of solidified ^3He . In addition, there exist many other methods of practical thermometry in the temperature range below 1 K (e.g. second sound in a $^3\text{He}-^4\text{He}$ mixture [21], superconducting transition fixed points of alloys and pure metals [32]). In the present work, a direct comparison of ITS-90 and PLTS-2000 from 0.65 K to 1 K has been performed for the first time. For this purpose, a vapour pressure thermometer and a melting pressure thermometer were installed on the same copper block and measured simultaneously. To check repeatability, the experiment was conducted twice, in 2019 and 2020. The results show that at 1 K, temperatures of ITS-90 (T_{90}) exceed those of PLTS-2000 (T_{2000}) by 0.28 mK; this difference increases to 1.58 mK at 0.65 K. Our results are consistent with those of an indirect comparison made at PTB in 2006 (differing by less than 0.22 mK). A new ^3He vapour-pressure equation was already proposed by Engert *et al* (2007) [16], which has the same mathematical form as that of ITS-90. To take the latest, more accurate data into account, only a slight adjustment of the coefficients might be necessary, since the current data agree very well with those of [15]. It is hoped this work will lead to a more accurate version of the equation used for this range in ITS-90.

Acknowledgments

This work was supported by the European Metrology Programme for Innovation and Research (EMPIR) Joint Research Project 18SIB02 Real-K 'Realising the redefined kelvin'. Changzhao Pan was supported by funding provided by a

Horizon 2020 Marie Skłodowska Curie Individual Fellowship 2018 (No. 834024). This work was developed within the framework of the European Metrology Research Program (EMRP) joint research project ‘SIB01 InK: Implementing the new kelvin’. The EMRP is jointly funded by the EMRP participating countries within EURAMET and the European Union. The authors thank Prof. Bogumil Jeziorski for kindly supplying the second virial coefficient of ^3He for temperatures below 1 K. They are also grateful to Prof. Carlo Beenakker of the University of Leiden for providing the text of reference [5].

ORCID iDs

Changzhao Pan  <https://orcid.org/0000-0002-1473-2582>
 Fernando Sparasci  <https://orcid.org/0000-0002-9130-4338>
 Mark Plimmer  <https://orcid.org/0000-0001-8727-2997>
 Bo Gao  <https://orcid.org/0000-0002-7277-5150>
 Laurent Pitre  <https://orcid.org/0000-0001-9885-7544>

References

- [1] Preston-Thomas H 1990 The international temperature scale of (ITS-90) *Metrologia* **27** 3–10
- [2] BIPM 2001 *Procès-Verbaux des Séances du Comité International des Poids et Mesures* vol 68(Sèvres: BIPM) pp 128–30
- [3] Rusby R L, Durieux M, Reesink A L, Hudson R P, Schuster G, Kühne M, Fogle W E, Soulen R J and Adams E D 2002 *J. Low Temp. Phys.* **126** 633–42
- [4] Rusby R L and Swenson C A 1980 *Metrologia* **16** 73–87
- [5] El Samahy A E 1979 Thermometry between 0.5 K and 30 K *PhD Thesis* University of Leiden (unpublished)
- [6] Berry K H 1979 NPL-75: A low temperature gas thermometry scale from 2.6 K to 27.1 K *Metrologia* **15** 89–115
- [7] Soulen R J, Fogle W E and Colwell J H 1994 Measurements of absolute temperature below 0.75 K using a Josephson-junction noise thermometer *J. Low Temp. Phys.* **94** 385–487
- [8] Schuster G and Hechtfisher D 1992 Extrapolation of ITS-90 to lower temperatures, in *Temperature, its Measurement and Control in Science and Industry* vol 6 ed J F Schooley (New York: American Institute of Physics) pp 97–100
- [9] Ni W, Xia J S, Adams E D, Haskins P S and McKisson J E 1995 ^3He Melting pressure temperature scale below 25 mK *J. Low Temp. Phys.* **99** 167–82
- [10] Meyer C and Reilly M 1996 Realization of the ITS-90 at the NIST in the range 0.65 K to 5.0 K using the ^3He and ^4He vapour-pressure thermometry *Metrologia* **33** 383–9
- [11] De Groot M J 1997 The measurement of the helium vapour pressure between 0.53 K and 1 K *Proc. of the IMEKO Conf. on Low Temperature Thermometry and Dynamic Temperature Measurement* pp L104–9
- [12] Hill K D 2002 Realizing the ITS-90 below 4.2 K at the National Research Council of Canada *Metrologia* **39** 41–9
- [13] Shimazaki T and Tamura O 2003 Realization of the ^3He vapour-pressure temperature scale at NMIJ/AIST *AIP Conf. Proc.* **684** 119–24 American Institute of Physics
- [14] Shimazaki T, Toyoda K and Tamura O 2011 Realization of the ^3He vapor-pressure temperature scale and development of a liquid-He-free calibration apparatus *Int. J. Thermophys.* **32** 2171–82
- [15] Fellmuth B, Hechtfisher D and Hoffmann A 2003 PTB-96: The ultra-low temperature scale of PTB, in *CP684 Temperature: Its Measurement and Control in Science and Industry* vol 7 ed D C Ripple (New York: American Institute of Physics) pp 71–6
- [16] Engert J, Fellmuth B and Jousten K 2007 A new ^3He vapour-pressure based temperature scale from 0.65 K to 3.2 K consistent with the PLTS-2000 *Metrologia* **44** 40–52
- [17] Schuster G, Hoffmann A and Hechtfisher D 2005 *PTB-96, the Ultra-low Temperature Scale of PTB* (Braunschweig: PTB-Bericht) PTB-Th-2
- [18] Engert J, Heyer D and Fischer J 2013 Low-temperature thermometry below 1 K at PTB *AIP Conf. Proc.* **1552** 136–41 American Institute of Physics
- [19] Peruzzi A and De Groot M J 2003 Evaluation of uncertainty in the realization of the provisional low temperature scale from 10 mK to 1 K at NMI *Proc. of the Int. Conf. on the Uncertainty of Measurement UNCERT (Oxford, UK, 9-10 April 2003)*
- [20] Pitre L, Hermier Y and Bonnier G 2003 The realization of the provisional low temperature scale of 2000 at BNM-INM *AIP Conf. Proc.* **684** 95–100 American Institute of Physics
- [21] Pitre L, Hermier Y and Bonnier G 2003 The comparison between a second-sound thermometer and a melting-curve thermometer from 0.8 K down to 20 mK *AIP Conf. Proc.* **684** 101–6 American Institute of Physics
- [22] Nakagawa H 2016 Realization of PLTS-2000 for low-temperature resistance thermometer calibration services below 650 mK *Int. J. Thermophys.* **37** 112
- [23] Sparasci F, Pitre L, Truong D, Risegari L and Hermier Y 2011 Realization of a ^3He - ^4He vapor-pressure thermometer for temperatures between 0.65 K and 5 K at LNE-CNAM *Int. J. Thermophys.* **32** 139–52
- [24] Schuster G and Hoffmann A 1997 Construction and test of ^3He melting pressure sensors *EC Project Report Contract no. SMT4-CT96-2052* PTB, Germany
- [25] Pavese F and Molinar G 1992 *Modern Gas-Based Temperature and Pressure Measurements* (New York: Plenum Press)
- [26] Rusby R L, Fellmuth B, Engert J, Fogle W E, Adams E D, Pitre L and Durieux M 2007 Realization of the ^3He melting pressure scale, PLTS-2000 *J. Low Temp. Phys.* **149** 156–75
- [27] Hurly J J and Moldover M R 2000 *Ab initio* values of the thermophysical properties of helium as standards *J. Res. Natl. Inst. Stand. Technol.* **105** 667–88
- [28] Al-Maaitah A F, Sandouqa A S, Joudeh B R and Ghassib H B 2017 Thermodynamic properties of spin-polarized ^3He gas in the temperature range 1 mK–4 K from the quantum second virial coefficient *Int. J. Mod. Phys. B* **31** 1750202
- [29] Czachorowski P et al 2020 Second virial coefficients for ^4He and ^3He from an accurate relativistic interaction potential *Phys. Rev. A* **102** 042810
- [30] Fellmuth B, Engert J, Shimazaki T and Sparasci F 2018 Guide to the realization of the ITS-90 Vapour Pressure Scales and Pressure Measurements (Sèvres: Bureau International des Poids et Mesures) ch 3 p 22
- [31] Lounasmaa O V 1974 *Experimental Principles and Methods below 1 K* (London: Academic)
- [32] Schöttl S et al Evaluation of SRD1000 superconductive reference devices 2005 *J. Low Temp. Phys.* **138** 941–6